Identifying intrasulcal medial surfaces for anatomically consistent reconstruction of the cerebral cortex

Sergey Osechinskiy and Frithjof Kruggel

Department of Biomedical Engineering, University of California, Irvine, CA 92697, USA

ABSTRACT

A novel approach to identifying poorly resolved boundaries between adjacent sulcal cortical banks in MR images of the human brain is presented. The algorithm calculates an electrostatic potential field in a partial differential equation (PDE) model of an inhomogeneous dielectric layer of gray matter that surrounds conductive white matter. Correspondence trajectories and geodesic distances are computed along the streamlines of the potential field gradient using PDEs in a Eulerian framework. The skeleton of a sulcal medial boundary is identified by a simple procedure that finds irregularities/collisions in the field of correspondences. The skeleton detection procedure is robust to noise, does not produce spurious artifacts and does not require tunable parameters. Results of the algorithm are compared with a closely related technique, called Anatomically Consistent Enhancement (ACE) (Han et al. CRUISE: Cortical reconstruction using implicit surface evolution, 2004). Results demonstrate that the approach proposed here has a number of advantages over ACE and produces skeletons with a more regular structure. This algorithm was developed as a part of a more general PDE-based framework for cortical reconstruction, which integrates the potential field gradient flow and the skeleton barriers into a level set deformable model. This technique is primarily aimed at anatomically consistent and accurate reconstruction of cortical surface models in the presence of imaging noise and partial volume effects, but the identified intrasulcal medial surfaces can serve other purposes as well, e.g. as landmarks in nonrigid registration, or as sulcal ribbons that characterize the cortical folding.

Keywords: Segmentation, Cerebral cortex, Cortical Reconstruction, 3D Skeletonization

1. INTRODUCTION

Reconstruction of accurate cortical surface models from magnetic resonance (MR) images of the human brain is an important area of research in medical image analysis. Surface models serve as the basis for qualitative characterization of cortical folding patterns, as well as for quantitative measurement of cortical thickness. The reconstruction process is hindered by noise and partial volume effects (PVE) inherent in MR images, which may contribute to geometrical inaccuracies and topological errors in a surface representation, leading to anatomically incorrect results. Specifically, a layer of *pia mater* and cerebrospinal fluid (CSF), which separates the opposite banks of gray matter (GM) in deep narrow sulcal folds, is often poorly resolved due to limited spatial resolution and PVE. As a result, the cortical banks can appear fused together. This may lead to underestimation of the sulcal depth and overestimation of the cortical thickness, unless a reconstruction algorithm includes certain anatomically consistent constraints for implicit or explicit recovery of intrasulcal separation boundaries.

For example, cortical reconstruction algorithms based on surface mesh deformable models[1,2] typically use a smoothness constraint in conjunction with a mesh self-intersection check, benefiting from subvoxel precision of vertex position in mesh representation, and allowing an infinitesimally small separation between surfaces of the touching banks. In addition, a proximity constraint between two deformed surfaces can help locate the depths of the sulci.[2] The above constraints are examples of the implicit recovery of intrasulcal separation boundaries, since no model of a separating barrier is derived explicitly.

In level set based methods, self-intersections of an interface are not an issue, but the topology of a surface in level set representation can, in general, be changed freely during evolution, therefore an entire section of a surface between touching banks of GM can vanish. Two known approaches address this problem and serve as

Send correspondence to Sergey Osechinskiy at sosechin@uci.edu.

Medical Imaging 2011: Image Processing, edited by Benoit M. Dawant, David R. Haynor,
Proc. of SPIE Vol. 7962, 79620N · © 2011 SPIE · CCC code: 1605-7422/11/$18 · doi: 10.1117/12.877863

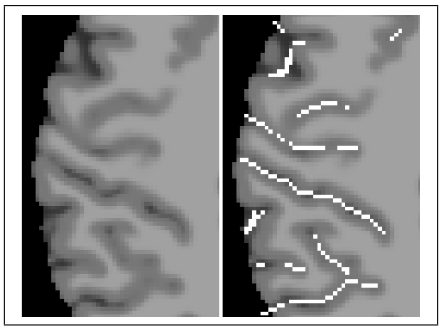

Figure 1. Illustration of a brain slice fragment. The skeleton (white pixels) marks a separation boundary between gray matter banks, which are fused together at some locations.

examples of the implicit recovery of intrasulcal separation boundaries. Zeng et al.[3] described a coupled surface propagation algorithm, where a thickness constraint controls the maximal separation between the inner and outer surface, and thus detects cases of buried cortex within the sulcal folds. Han et al.[4,5] proposed a topology-preserving geometric deformable model that combines a level set method with a constraint on digital topology. The topological constraint solves the problem of the touching banks, which would otherwise create a change in topology (e.g., a tunnel), but does not resolve cases of fully buried cortex, which do not yield any topological changes. To address this, Han et al. augmented their method with the Anatomically Consistent Enhancement (ACE) procedure[4,6] that explicitly finds separation barriers between sulcal GM banks in the form of a digital skeleton (Fig. 1). ACE extracts the intrasulcal skeleton as shocks in the weighted-distance transform, which is obtained by solving the Eikonal equation with a speed function modulated by the presence of CSF.

Apart from their usefulness in cortical surface reconstruction exemplified by ACE, intrasulcal medial surfaces can serve as distinct anatomical features characterizing the cortical folding. Zeng et al.[7] described an approach for finding a parametric representation of a thin three-dimensional (3D) ribbon embedded in a sulcus. The algorithm requires a model of the outer cortical surface and obtains each sulcal ribbon through the process of active contour deformation, which requires manual initialization and may be computationally expensive. In their study of cortical folding, Mangin et al.[8] pointed to a number of problems pertaining to deformable contours approaches, and used a different approach, which involved skeletonization of the white matter (WM) object complement in sulci (GM and CSF union). Mangin et al. noted[8] that skeletonization by conventional thinning approaches can be very sensitive to noise, which justified the development of their robust homotopic skeletonization algorithm with built-in topological and regularization constraints.[8,9]

We propose a novel algorithm for explicit extraction of intrasulcal medial surfaces that separate the banks of GM in sulci in an anatomically consistent way. Of all the methods cited above, our approach is most closely related to that of Han et al.,[6] but uses a different mathematical model. Our algorithm calculates a potential field outside of WM by using an inhomogeneous dielectric model with the permittivity spatially modulated by the GM content. Correspondence trajectories and geodesic distances are computed along the lines of the gradient of the potential field. The medial surface skeleton is identified from the distance field and/or the field of correspondence trajectories. These steps are integrated in our PDE-based framework for cortical reconstruction, which is described in our previous work.[10] This paper introduces a new improved procedure for robust intrasulcal medial surface skeleton detection that is based on finding the irregularities in the field of correspondence trajectories. The new procedure has a number of advantages over other previously published approaches,[6,10] and is particularly robust with respect to misclassifications of voxel tissue class membership, as demonstrated by the cross-method comparison of results on simulated and real MR images.

2. METHODS

Our algorithm uses as input the following 3D data sets derived from a source MR image: 1) WM and GM tissue class membership/probability images, $P_w(\vec{r})$ and $P_g(\vec{r})$; 2) an edited segmentation of WM, $B_w(\vec{r})$ ($\vec{r} \in \Omega$). Here, $\vec{r} = (x, y, z)$ denotes a point in the 3D space $\mathbb{R}^3$, $\Omega \subset \mathbb{R}^3$ denotes the image domain with the boundary $\Gamma(\Omega)$,

and all data are sampled at discrete locations of the voxel grid. The edited segmentation of WM refers to a WM core object that has been automatically or manually preprocessed/edited for the purpose of refining the WM topology: filling of ventricles and sub-cortical structures,[11] fixing of topological defects, etc. The $B_w(\vec{r})$ volume can be supplied in the form of a binary image, an edited class membership or a level set function; we will denote the binary domain of the WM core by Ω_w ($\Omega_w = \{\vec{r} \in \Omega | B_w(\vec{r}) = 1\}$). Image preprocessing, tissue classification, and WM segmentation/editing steps have been described elsewhere (e.g., see [6,11,12] for details). The tissue classification was performed by a modified version[12] of the adaptive fuzzy clustering algorithm (AFCM[13]) that included a spatial regularization term (see FANTASM[6]).

The algorithm consists of the following stages: 1) a potential field is calculated as a solution to an electrostatic PDE model, where GM is posing as an inhomogeneous dielectric layer that surrounds a conductive WM object; 2) correspondence trajectories and geodesic distances from WM along the streamlines of the potential field gradient are computed in a set of PDEs in Eulerian framework; 3) a digital skeleton surface separating GM sulcal banks is identified through a search for irregularities in the field of correspondence trajectories.

2.1 Model of the potential field

The potential field is found as a solution of Maxwells equation for an electric field inside inhomogeneous dielectric medium in the absence of free charges:

$$\nabla(\varepsilon(\vec{r})\vec{E}(\vec{r})) = \nabla\varepsilon\nabla\varphi + \varepsilon\Delta\varphi = 0, \tag{1}$$

where φ is the potential and ε is the permittivity that depends on GM tissue class probability value (ε is close to $\varepsilon_{max} >> 1$ in pure GM, and is 1 in CSF). The idea behind this model is that the flux of the electric field will be concentrated in regions of higher permittivity – that is, where GM class probability is higher – therefore trajectories following the lines of the electric field will trace through the GM layer before exiting into the surrounding space. The potential field ϕ is found as a steady state solution of a corresponding nonstationary partial differential equation (PDE):

$$\frac{\partial\varphi}{\partial t} = \nabla\varepsilon\nabla\varphi + \varepsilon\Delta\varphi. \tag{2}$$

Equation (2) can also be viewed as an inhomogeneous diffusion equation, where $\varepsilon(\vec{r})$ is a spatially varying diffusion coefficient proportional to GM class probability. It is expected that a substance will diffuse more freely in GM, therefore the lines of the field φ will tend to concentrate in the GM compartment. The equation (2) is discretized[14] and solved by the iterative Jacobi scheme[15] with boundary conditions $\varphi(\vec{r}) = 1 : \vec{r} \in \Omega_w$, and $\varphi(\vec{r}) = 0 : \vec{r} \in \Gamma(\Omega)$.

2.2 Distance field and correspondence trajectories

Lines of the field gradient $\nabla\varphi$, originating at the WM/GM interface and tracing through the GM layer and beyond, form the correspondence trajectories, which associate each outer location with a source point at the interface. There is a close analogy with a gradient field of a harmonic function in the Laplacian measure of cortical thickness,[16] which gains popularity because of its favorable anatomical properties. In the Laplacian method, both the inner WM/GM and the outer pial GM surface are presumed to be known, and the harmonic field ($\Delta\phi = 0$) is computed between the two surfaces; mapping by the gradient field forms a one-to-one correspondence. In our model, only the inner surface is known, and the correspondence breaks down where the trajectories collide, e.g., between two cortical banks in a sulcus. Instead of explicitly finding and integrating trajectory lines in a Lagrangian framework, we compute the correspondence functions $\vec{\psi} = [\psi_1(\vec{r}), \psi_2(\vec{r}), \psi_3(\vec{r})]$ and the geodesic distance function $d(\vec{r})$ in the Eulerian PDE approach,[16,17] which allows a "fast marching" implementation as efficient as fast marching solvers for the Eikonal equation[18,19] (see also ACE[6]). Using the method,[17] the distance field can be found as a solution of a PDE on a fixed grid:

$$\frac{\nabla\varphi}{||\nabla\varphi||} \cdot \nabla d(\vec{r}) = 1, \tag{3}$$

with the boundary condition $d(\vec{r} \in \Gamma(\Omega_w)) = 0$. Correspondence functions $\vec{\psi}$, which establish a correspondence between a point in the field domain $\vec{r} \in \Omega \backslash \Omega_w$ and a "source" point in the WM boundary $\vec{\psi} \in \Gamma(\Omega_w)$, can be found as solutions of the following PDE:[16]

$$\frac{\nabla \varphi}{||\nabla \varphi||} \cdot \nabla \psi_i(\vec{r}) = 0, \tag{4}$$

with boundary conditions $\psi_i\left(\vec{r} = [x_1, x_2, x_3] \in \Gamma(\Omega_w)\right) = x_i$, where $i = 1, 2, 3$.

2.3 Extraction of the skeleton of intrasulcal medial surfaces

A skeleton of the surfaces separating cortical banks in sulci (Fig. 1) can be identified by numerically evaluating the gradient's magnitude $||\nabla d||$ and finding shocks, or singularities of the distance field, in an analogous manner to the procedure of the ACE method.[6] This approach, however, requires an empirically defined threshold parameter T on values of $||\nabla L_0||$ ($T < 1$, e.g. $T = 0.8$), and a somewhat arbitrarily defined minimum cut-off distance from the WM/GM interface (for details, see[4,6]). The method can be sensitive to noise, and may yield extraneous branches in the skeleton if the interface is not smooth. We propose a more reliable skeleton detection algorithm, which takes advantage of the correspondence functions $\vec{\psi}(\vec{r})$ and requires less parameters. For each point $\vec{r_i}$ in the domain, the algorithm finds the maximal Euclidean distance between correspondence functions in a 6-connected neighborhood $\vec{r_j} \in N_i$, $D = \max_j \left|\left|\vec{\psi}(\vec{r_i}) - \vec{\psi}(\vec{r_j})\right|\right|$. Since correspondences encode coordinates of points of origin on the WM/GM interface, a large value of distance D signifies that correspondence trajectories converge in the neighborhood of $\vec{r_i}$; such points can be classified as belonging to the skeleton. The identified skeleton can be used to guide a cortical reconstruction algorithm in places where the boundary between cortical banks is otherwise not clearly detectable (Fig. 1). For further visualization or use in the analysis of cortical folding, the skeleton can be post-processed into a 3D ribbon model of intrasulcal medial surfaces: for example, morphologically thinned, bounded by a convex hull of the brain, separated into connected components, filtered from small components, labeled by a sulcal basin labeling algorithm,[20] and tessellated into a mesh.

3. RESULTS AND DISCUSSION

The algorithm was evaluated on simulated sulci with a simplified geometry, and on real MR images of the human brain from the Open Access Series of Imaging Studies (OASIS) repository.[21,22]

Synthetic 3D test images simulate a WM core with a deep U-shaped trough (a "sulcus" between two "gyral stalks"), overlaid by a layer of GM that has unequal thickness at the opposite banks inside the trough (Fig. 2). The curvature radius of a sulcal trough and gyral stalk is 10 mm. In some test cases, the two cortical banks are fully separated by the background, and in other cases, they are fused at the fundus ("buried" cortex or unresolved fundus) or in the periphery ("fused banks"). It can be seen that the method is capable of reconstructing the boundary surface separating the two cortical banks, and finds a geometrically plausible solution in incompletely resolved cases. Side-by-side comparison of results of our method and those of ACE in Fig. 2 shows that skeletons produced by our method have a more regular structure, whereas skeletons produced by ACE can have small extraneous branches and some discontinuities. Our method does not produce spurious detections very close to the WM/GM border, and thus does not require a minimum distance cut-off parameter, which is needed in ACE (for illustration, ACE results in the bottom row of Fig. 2 were produced without such minimum distance cut-off, and thus demonstrate small white strokes of spurious detection near WM fundus).

Our method is significantly more robust with respect to tissue classification errors resulting from the noise in an MR image, as illustrated in Fig. 3 by test cases, where class membership data were corrupted by different levels of uniformly distributed noise, simulating voxel misclassifications. Skeletons produced by our method (Fig. 3, top row) show very little degradation, while ACE skeletons (Fig. 3, bottom row) are significantly affected and increasingly exhibit spurious strokes. Although the tested level of noise in the class images is exaggerated, it clearly emphasizes the advantage and robustness of the new method. Improved robustness to noise of a diffusion based approach compared to an Eikonal equation based approach was previously demonstrated in the context of 2D image segmentation.[23] The advantage of a diffusion based method can be explained by the ability of a diffusive process to propagate information around a misclassified voxel, thus taking advantage of the spatial

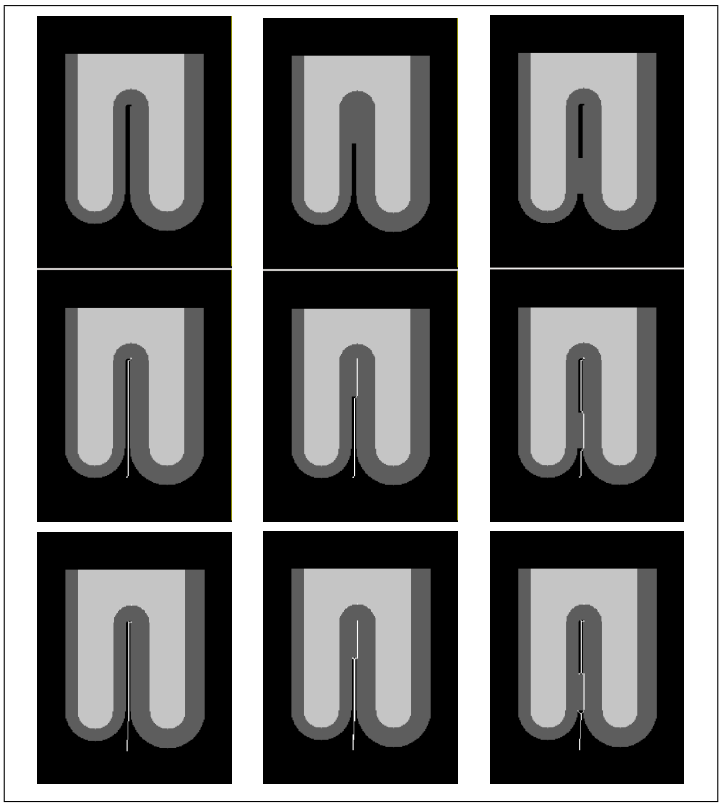

Figure 2. Cross-sections of simulated test images (left: fully resolved sulcus; middle: unresolved fundus; right: bridged sulcus; the white line shows the location of the identified sulcal medial surface skeleton). Comparison of our method results (middle row) vs. ACE (bottom row; small spurious components are visible at the fundus because, for illustration purposes, no minimum distance cut-off filtering was used).

neighborhood, whereas a fast marching process in the Eikonal approach "marches straight through" that voxel, disregarding the spatial neighborhood.

The algorithm was applied to typical 1.5 Tesla T1-weighted MR images with 1.0 mm^3 voxel resolution (from the OASIS database). PDE computations were performed at sub-voxel (0.5 mm) grid spacing for better spatial resolution of skeletonized surfaces. The results of our method and ACE are shown side by side in Fig. 4. Overall, the results of the two methods are in good agreement, but it can be seen that skeletons produced by our method are, in general, smoother and have a more regular structure. The sulcal ribbons produced by ACE can have some holes and have more irregular surfaces compared to our results. Our method again demonstrated a significantly better robustness with respect to simulated noise added to the class images (Fig. 5). The overall running time for our method is 5-7 min per one hemisphere on a 2.6GHz AMD64 CPU, compared to less than 1 min for ACE. The computational time of algorithmic steps described in Sections 2.2 and 2.3 is close to that of the ACE method, as would be expected for similar fast marching implementation schemes. Compared to ACE, calculation of a PDE solution in Section 2.1 takes additional time. However, in our cortical reconstruction framework this additional invested time is regained later, when the computed potential field is re-used in a deformable model.

4. CONCLUSION

We presented a new method for anatomically consistent detection of intrasulcal separation boundaries in MR images. Our method synthesizes known image processing methods into a novel technique, which offers a number of advantages over previously published approaches. The identified intrasulcal medial surfaces can serve the following purposes: 1) editing of GM membership values for the emphasis of sulcal cortical bank boundaries in cortical segmentation; 2) constraining a cortical reconstruction deformable model at the cortical bank boundaries

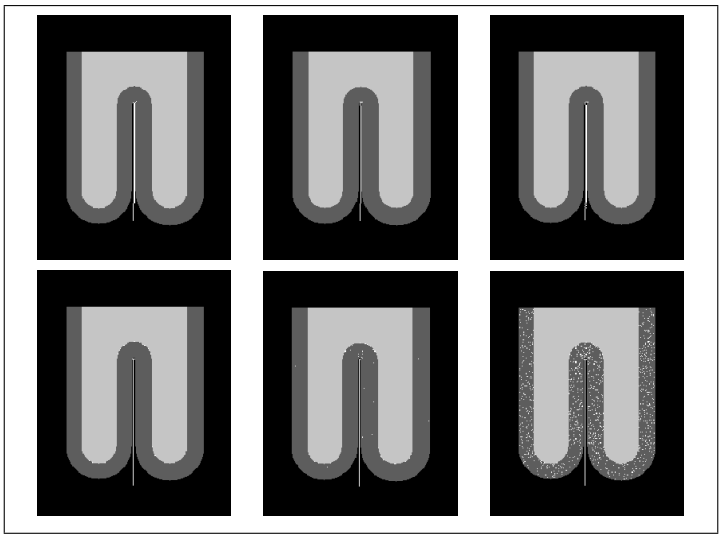

Figure 3. Comparison of our method results (top row) vs. ACE (bottom row) at different simulated noise levels in the WM, GM, CSF class images (left to right: noise level 0.2, 0.5, and 0.7; class membership values ranging from 0 to 1.0).

inside sulci; 3) deriving sulcal ribbon landmarks for a hybrid intensity and landmark based inter-subject nonrigid registration; 4) using sulcal ribbon anatomical features for characterization of cortical folding.

ACKNOWLEDGMENTS

We gratefully acknowledge the Open Access Series of Imaging Studies (OASIS) project for providing MRI data sets. The OASIS project is made available by Dr. Randy Buckner at the Howard Hughes Medical Institute (HHMI) at Harvard University, the Neuroinformatics Research Group (NRG) at Washington University School of Medicine, and the Biomedical Informatics Research Network (BIRN).

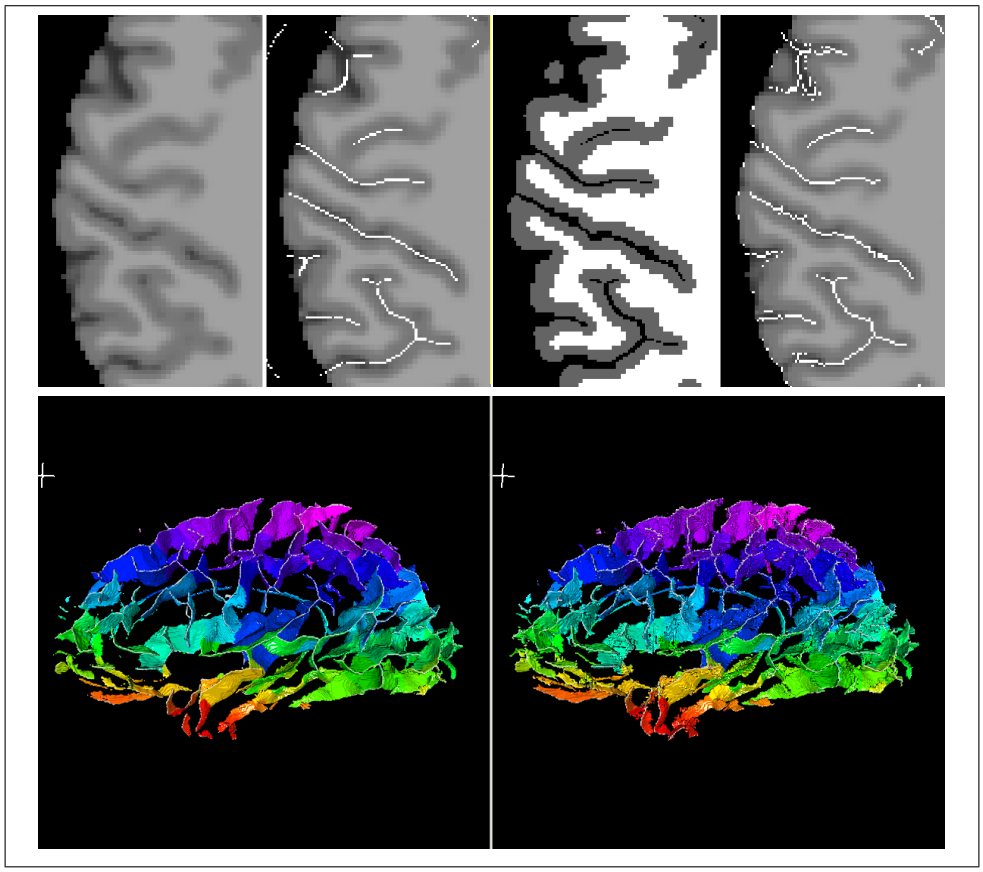

Figure 4. Top: fragment of an axial slice of a brain image (left to right: source image; image overlayed with the skeleton from our method; binarized cortical segmentation; image overlayed with the ACE skeleton). Bottom: 3D rendering of intrasulcal medial surfaces from our method (left) and from ACE (right), color-coded with sulcal basin labels for better visualization.

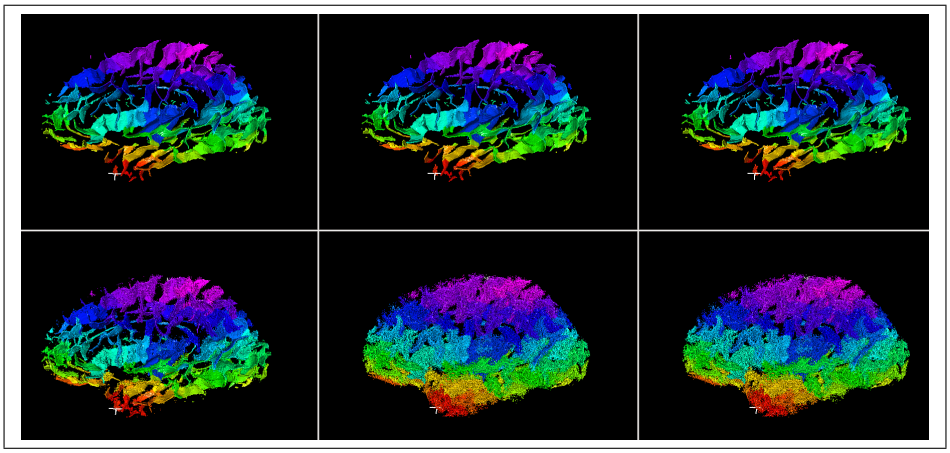

Figure 5. A 3D rendering of intrasulcal medial surfaces comparing our results (top row) to ACE (bottom row) at different simulated noise levels in the WM, GM, CSF class images (left to right: noise level 0.2, 0.5, and 0.7; class membership values ranging from 0 to 1.0). Sulcal ribbons are color-coded with sulcal basin labels for better visualization.

REFERENCES

[1] MacDonald, D., Avis, D., and Evans, A. C., "Proximity constraints in deformable models for cortical surface identification," *LNCS (MICCAI'98)* **1496**, 650–659 (1998).

[2] Dale, A. M., Fischl, B., and Sereno, M. I., "Cortical surface-based analysis: I. segmentation and surface reconstruction," *NeuroImage* **9**(2), 179–194 (1999).

[3] Zeng, X., Staib, L., Schultz, R., and Duncan, J., "Segmentation and measurement of the cortex from 3-D MR images using coupled-surfaces propagation," *IEEE Trans. Med. Imag.* **18**(10), 927–937 (1999).

[4] Han, X., Xu, C., Tosun, D., and Prince, J. L., "Cortical surface reconstruction using a topology preserving geometric deformable model," *Proc. IEEE (MMBIA'01)*, 213–220 (2001).

[5] Han, X., Xu, C., and Prince, J. L., "A topology preserving level set method for geometric deformable models," *IEEE Trans. Patt. Anal. Mach. Intell.* **25**(6), 755–768 (2003).

[6] Han, X., Pham, D. L., Tosun, D., Rettmann, M. E., Xu, C., and Prince, J. L., "CRUISE: Cortical reconstruction using implicit surface evolution," *NeuroImage* **23**, 997–1012 (2004).

[7] Zeng, X., Staib, L., Schultz, R., Tagare, H., Win, L., and Duncan, J., "A new approach to 3D sulcal ribbon finding from MR images," *LNCS (MICCAI'99)* **1679**, 148–158 (1999).

[8] Mangin, J.-F., Frouin, V., Bloch, I., Régis, J., and López-Krahe, J., "From 3D magnetic resonance images to structural representations of the cortex topography using topology preserving deformations," *J. Math. Imaging Vis.* **5**(4), 297–318 (1995).

[9] Mangin, J.-F., Rivire, D., Cachia, A., Duchesnay, E., Cointepas, Y., Papadopoulos-Orfanos, D., Scifo, P., Ochiai, T., Brunelle, F., and Rgis, J., "A framework to study the cortical folding patterns," *NeuroImage* **23**(S1), S129–S138 (2004).

[10] Osechinskiy, S. and Kruggel, F., "PDE-based reconstruction of the cerebral cortex from MR images," *Proc. IEEE (EMBC'10)*, 4278–4283 (2010).

[11] Han, X., Xu, C., Rettmann, M. E., and Prince, J. L., "Automatic segmentation editing for cortical surface reconstruction," *Proc. SPIE* **4322**, 194–203 (2001).

[12] Kruggel, F., Brückner, M. K., Arendt, T., Wiggins, C. J., and von Cramon, D. Y., "Analyzing the neocortical fine-structure," *Med. Image Anal.* **7**, 251–264 (2003).

[13] Pham, D. and Prince, J., "Adaptive fuzzy segmentation of magnetic resonance images," *IEEE Trans. Med. Imag.* **18**(9), 737–752 (1999).

[14] Gerig, G., Kubler, O., Kikinis, R., and Jolesz, F., "Nonlinear anisotropic filtering of MRI data," *IEEE Trans. Med. Imag.* **11**(2), 221–232 (1992).

[15] Press, W. H., Teukolsky, S. A., Vetterling, W. T., and Flannery, B. P., [*Numerical Recipes in C++: The Art of Scientific Computing*], Cambridge University Press (2002).

[16] Rocha, K. R., Yezzi, A. J., and Prince, J. L., "A hybrid Eulerian-Lagrangian approach for thickness, correspondence, and gridding of annular tissues," *IEEE Trans. Imag. Proc.* **16**(3), 636–648 (2007).

[17] Yezzi, A. and Prince, J. L., "A PDE approach for measuring tissue thickness," *Proc. IEEE (CVPR'01)*, 87–92 (2001).

[18] Sethian, J., "A fast marching level set method for monotonically advancing fronts," *Proc. Natl. Acad. Sci.* **93**(4), 1591–1595 (1996).

[19] Osher, S. and Fedkiw, R. P., [*Level set methods and dynamic implicit surfaces*], Springer, New York (2002).

[20] Kruggel, F. and von Cramon, D. Y., "Measuring the cortical thickness," *Proc. IEEE (MMBIA'00)*, 154–161 (2000).

[21] Marcus, D. S., Wang, T. H., Parker, J., Csernansky, J. G., Morris, J. C., and Buckner, R. L., "Open access series of imaging studies (OASIS): Cross-sectional MRI data in young, middle aged, nondemented, and demented older adults," *J. Cogn. Neurosc.* **19**(9), 1498–1507 (2007).

[22] [*The Open Access Series of Imaging Studies (OASIS)*] (2011). http://www.oasis-brains.org/.

[23] Alvino, C., Unal, G., Slabaugh, Greg andPeny, B., and Fang, T., "Efficient segmentation based on eikonal and diffusion equations," *Int. J. Comp. Math.* **84**(9), 1309–1324 (2007).